International Journal of Bifurcation and Chaos, Vol. 26, No. 14 (2016) 1650233 (11 pages)

DOI: 10.1142/S0218127416502333

Crisis in Amplitude Control Hides in Multistability

Chunbiao Li*
Jiangsu Key Laboratory of Meteorological Observation and Information Processing, Nanjing University of Information Science and Technology, Nanjing 210044, P. R. China
School of Electronic and Information Engineering, Nanjing University of Information Science and Technology, Nanjing 210044, P. R. China
goontry@126.com
chunbiaolee@nuist.edu.cn

Julien Clinton Sprott
Department of Physics, University of Wisconsin-Madison, Madison, WI 53706, USA
sprott@physics.wisc.edu

Hongyan Xing
Jiangsu Key Laboratory of Meteorological Observation and Information Processing, Nanjing University of Information Science and Technology, Nanjing 210044, P. R. China
School of Electronic and Information Engineering, Nanjing University of Information Science and Technology, Nanjing 210044, P. R. China
xinghy@nuist.edu.cn

Received May 15, 2016; Revised September 10, 2016

A crisis of amplitude control can occur when a system is multistable. This paper proposes a new chaotic system with a line of equilibria to demonstrate the threat to amplitude control from multistability. The new symmetric system has two coefficients for amplitude control, one of which is a partial amplitude controller, while the other is a total amplitude controller that simultaneously controls the frequency. The amplitude parameter rescales the basins of attraction and triggers a state switch among different states resulting in a failure of amplitude control to the desired state.

Keywords: Amplitude control; Lyapunov exponents; multistability; basins of attraction.

*Author for correspondence

1. Introduction

The properties of chaos such as the determinacy of a chaotic system, the intrinsic randomness of chaotic signals, and the sensitivity to initial conditions of a chaotic phase trajectory have attracted intensive interest from physicists and engineers, and consequently the study of the dynamics of chaos has become one of the popular research topics in nonlinear dynamics. In order to apply a chaotic system to practical engineering, it is useful to design chaotic circuits [Yu *et al.*, 2011; Sprott, 2000, 2011] and synchronization methods [Chen *et al.*, 2012a, 2012b; Zhang & Yang, 2011, 2012]. However, the broadband spectrum of chaotic signals and the sensitivity to initial conditions pose a significant challenge to chaos amplifier design. Chaotic systems with an amplitude parameter provide the convenience of online amplitude adjustment. Chaotic systems with a constant Lyapunov exponent spectrum [Li & Wang, 2009; Li *et al.*, 2010; Li *et al.*, 2012] belong to this kind of system with an amplitude controller. Even the Lorenz system has one partial amplitude controller [Li & Sprott, 2013], showing that an amplitude parameter can be found even in systems with quadratic nonlinearities.

On the other hand, many systems are found with multistability whether in symmetric systems [Bao *et al.*, 2016; Xu *et al.*, 2016; Sprott, 2014; Sprott *et al.*, 2014; Li & Sprott, 2014a; Li *et al.*, 2015c] or asymmetric ones [Sprott *et al.*, 2013; Barrio *et al.*, 2009; Li *et al.*, 2016a, 2016b]. Sprott *et al.* pointed out that even a simple 3D asymmetric system can have coexisting point attractors, limit cycles, and strange attractors [Sprott *et al.*, 2013]. Amplitude control may be hindered by multistability because of the inevitable shrinking or expansion of the basins of attraction. The fixed or noisy initial conditions may walk across basin boundaries when a system is rescaled by an amplitude controller, and therefore any of the coexisting attractors may be triggered. This crisis of amplitude control also exists in chaotic systems with a single nonquadratic term in the presence of multistability [Li & Sprott, 2014b], where the Lyapunov exponents are linearly rescaled along with the frequency rather than invariable.

In this paper, in order to demonstrate the crisis hiding in multistability thoroughly, we have introduced a new multistable chaotic system that has two regimes of amplitude control with constant or linearly rescaled Lyapunov exponents. In Sec. 2, the chaotic system is described with some basic analysis. In Sec. 3, an exhaustive study of multistability is performed. In Sec. 4, two regimes of amplitude control are described, and the effect of multistability is demonstrated. Some conclusions and discussion are given in the last section.

2. A New System with a Line of Equilibria

As mentioned above, there are two different regimes of amplitude control. Some amplitude parameters rescale the signals without changing the Lyapunov exponents [Li & Wang, 2009; Li *et al.*, 2010; Li *et al.*, 2012; Li & Sprott, 2013], while others rescale the signals with linearly rescaled Lyapunov exponents [Li & Sprott, 2014b]. Some systems may have both classes of amplitude control. Such a system with two different parameters for amplitude control is

$$\begin{aligned} \dot{x} &= y + yz \\ \dot{y} &= yz - axz \\ \dot{z} &= bz^2 - y^2 \end{aligned} \tag{1}$$

The above system has six terms, five of which are quadratic and one of which is linear. There are two independent bifurcation parameters a and b, i.e. coefficients of two quadratic terms governing the dynamics of the system and leading to some bifurcations of the system. System (1) has two amplitude parameters, one of which is the coefficient of the linear term y in the first equation controlling the amplitude and frequency of all three signals, while the other is the coefficient of the term y^2 governing the amplitude of the variables x and y while leaving z unchanged. The dynamic behavior determined by the two bifurcation parameters a and b is shown in Fig. 1, giving an overall description of the dynamics.

The relatively large black dynamic regions in Fig. 1 show that system (1) has robust chaotic solutions. Specifically, for large a and small b, the system is chaotic, with limit cycles dominating at large b. The thin bands of light blue within the black chaotic region corresponds to periodic windows. When $a = 5.5, b = 0.55$, system (1) has a strange attractor as shown in Fig. 2. The Lyapunov exponents are $(0.1276, 0, -2.1728)$, and the corresponding Kaplan–Yorke dimension $D_{\mathrm{KY}} = 2.0587$ using the method of Wolf *et al.* [1985]. Compared with the newly developed Leonov method [Kuznetsov, 2016; Kuznetsov *et al.*, 2016; Leonov *et al.*, 2016],

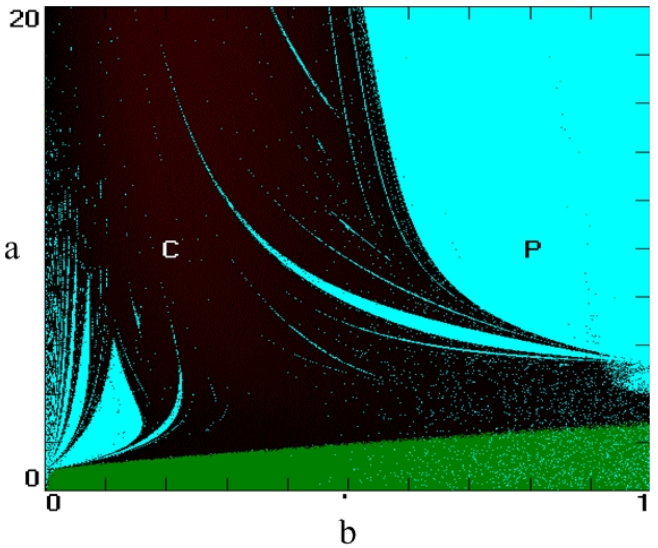

Fig. 1. Dynamic regions governed by the two bifurcation parameters a and b. The chaotic regions are shown in black, the periodic regions are shown in light blue, and the fixed point regions are shown in green.

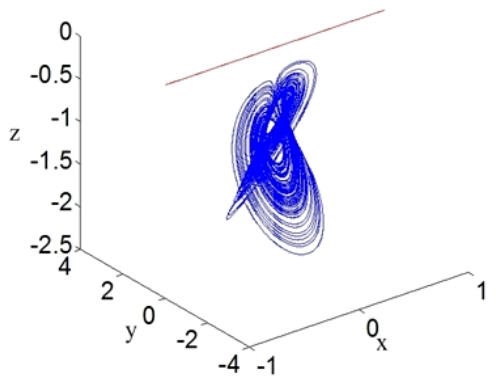

(a)

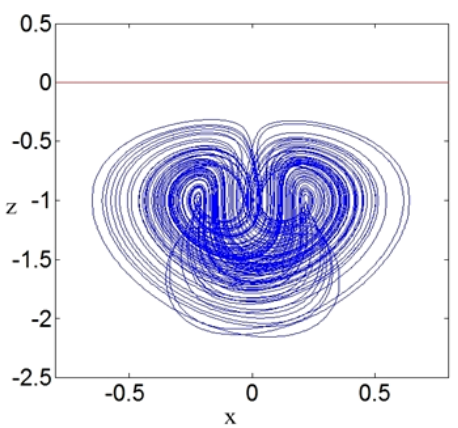

(b)

Fig. 2. Strange attractor at $a = 5.5, b = 0.55$ with initial conditions $(0, 0.4, -1)$. The red line is the line of equilibria.

the accuracy of the calculation of Lyapunov exponents by Wolf method depends on the time and initial conditions but both algorithms give the same identification for various states.

The system has a line of equilibria, $P_1 = (x, 0, 0)$ and two isolated equilibrium points, $P_{2,3} = (\pm 0.1348, \pm 0.7416, -1)$. The equilibria line lies outside the attractor rather than being surrounded by it [Jafari & Sprott, 2013]. The eigenvalues for the line equilibria are all zero, but further analysis shows that the system is nonlinearly unstable. This is different from the system LE1 [Jafari & Sprott, 2013], where the line equilibria have eigenvalues depending on the third-dimensional variable z and the basin of attraction for the strange attractor intersects the line equilibrium in some portions. Other chaotic systems like SL11 [Li & Sprott, 2014b] also have a line equilibria with the same stability, even systems AB5 and AB6 [Li *et al.*, 2015a] have two perpendicular lines of equilibria, however none of the systems like system (1) provide two regimes of amplitude control. The eigenvalues for the two isolated equilibrium points $P_{2,3}$ are $(-2.5817, 0.2408 \pm 1.5118i)$. One negative real value and a pair of complex conjugate eigenvalues with positive real parts indicate $P_{2,3}$ are saddle-foci with index 2. System (1) is unstable at all these equilibria, so the attractor is self-excited rather than hidden [Jiang *et al.*, 2016; Leonov *et al.*, 2011, 2012; Wei & Zhang, 2014; Wei *et al.*, 2014].

System (1) has rotational symmetry with respect to the z-axis as evidenced by its invariance under the coordinate transformation $(x, y, z) \to (-x, -y, z)$. When $b > 0$, three equilibrium points are: $P_1 = (x, 0, 0)$ and $P_{2,3} = (\frac{\pm\sqrt{b}}{a}, \pm\sqrt{b}, -1)$. The two isolated equilibrium points P_2 and P_3 are symmetric about the z-axis. Linearizing system (1) at the line equilibria $P_1 = (x, 0, 0)$ gives the Jacobian matrix

$$J_1 = \begin{pmatrix} 0 & 1+z & y \\ -az & z & y - ax \\ 0 & -2y & 2bz \end{pmatrix} = \begin{pmatrix} 0 & 1 & 0 \\ 0 & 0 & -ax \\ 0 & 0 & 0 \end{pmatrix}.$$

From $|\lambda I - J_1| = \lambda^3 = 0$, the three eigenvalues are all zero, so the system stability at the line equilibria depends on the nonlinear quadratic function, which may be analyzed by the method based on polar coordinates [Strogatz, 1994] or by numerical simulation. The second and third isolated equilibrium points $P_{2,3}$ are stable when $a < 2b + 1$ according to the stability criterion of Routh–Hurwitz with

characteristic equation $\lambda^3 + (2b + 1)\lambda^2 + 2b\lambda + 2ab = 0$, which leads to the green band on the bottom of the dynamic region in Fig. 1. In fact, when parameters (a, b) are selected in that area, the system can converge to either of the two stable point attractors depending on initial conditions.

3. Multistability Analysis

The three different colors in the dynamic regions of Fig. 1 indicate three different dynamics, i.e. point attractors, limit cycles, and strange attractors. Since each pixel in the plot uses a different random initial condition chosen from a Gaussian distribution with mean zero and variance 1.0, dotted areas indicate possible multistability or perhaps transient dynamics. Note that two attractors of the same type, such as two equilibrium points will have the same color since they have the same sign of the largest Lyapunov exponent. In fact, the system (1) has two basic multistability patterns, one of which shares the same Lyapunov exponents while the other corresponds to different exponents. As shown in Figs. 3 and 4, when the parameter a varies from 25 to 11, a symmetric pair of interlinked limit cycles evolve to chaos through respective period-doubling bifurcations and then merge into a single symmetric strange attractor.

As shown in Fig. 3, when there are two coexisting attractors, the average of the variable y is positive for one and negative for the other as shown in blue and red, respectively. When the two attractors merge into a single one, the average of signal

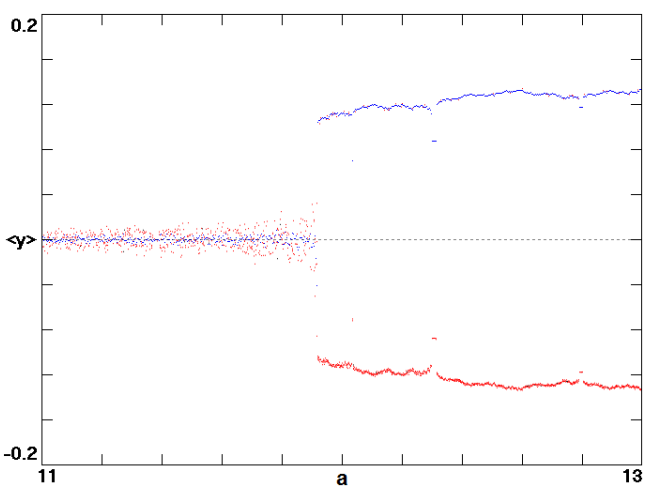

Fig. 3. A symmetric pair of coexisting attractors is distinguished by the average value of the variable y when a varies in $[11, 13]$ with initial conditions $(\pm 0.1, 0, -1)$.

y converges to zero. Figure 4 gives some details of the attractor merging. When $a = 25$, two limit cycles are interlinked and independently undergo a period-doubling bifurcation with a decrease of the parameter a. Two interlinked period-2 limit cycles appear at $a = 20$, and they individually undergo additional period-doublings until two interlinked strange attractors appear at $a = 14$. With further decrease of parameter a, the two interlinked attractors expand further with an edge collision (the edges of basins of attraction for coexisting attractors intertwine violently and finally basins get connected to be a unity inevitably), at which point they merge into a single symmetric strange attractor around $a = 11.9$.

The basin of attraction provides another way to visualize the two attractors. The basins will vary with the system parameters. Different basins of attraction will merge or split, when the attractors merge or a new attractor is born. A symmetric pair of coexisting attractors usually reside in symmetric basins. Figure 5 shows a cross-section of the basins for $z = -1$ (which contains the isolated equilibria) with $a = 13, b = 0.55$ where the system has a symmetric pair of strange attractors whose cross-sections are shown in black. Note the fractal structure of the basin boundary.

When the parameter a decreases further, the solution converges to a symmetric pair of point attractors as indicated by the green region at the bottom of Fig. 1. In the opposite direction, when the parameter a increases, the two interlinked limit cycles contract and merge into a single symmetric limit cycle as shown in Fig. 6. Thereafter, a further increase of the parameter a does not alter the periodic oscillation and does not change the amplitude of the variable y while only causing a slight change in the amplitude of the variables x and z, giving a robust periodic oscillation.

Furthermore, system (1) has other regions of multistability such as coexisting point attractors and limit cycles coexisting with strange attractors. As shown in Fig. 7(a), when $a = 1, b = 0.1$, two stable point attractors at $P_{2,3} = (\pm 0.3162, \pm 0.3162, -1)$ coexist with the same eigenvalues $(-1.1747, -0.0127 \pm 0.4124i)$ and Lyapunov exponents $(-0.0105, -0.0159, -1.1660)$. As shown in Fig. 7(b), when $a = 5$, $b = 0.95$, a chaotic attractor coexists with a limit cycle with corresponding Lyapunov exponents $(0.0717, 0, -2.2854)$ and $(0, -0.0085, -2.7586)$ and Kaplan–Yorke dimensions 2.0314

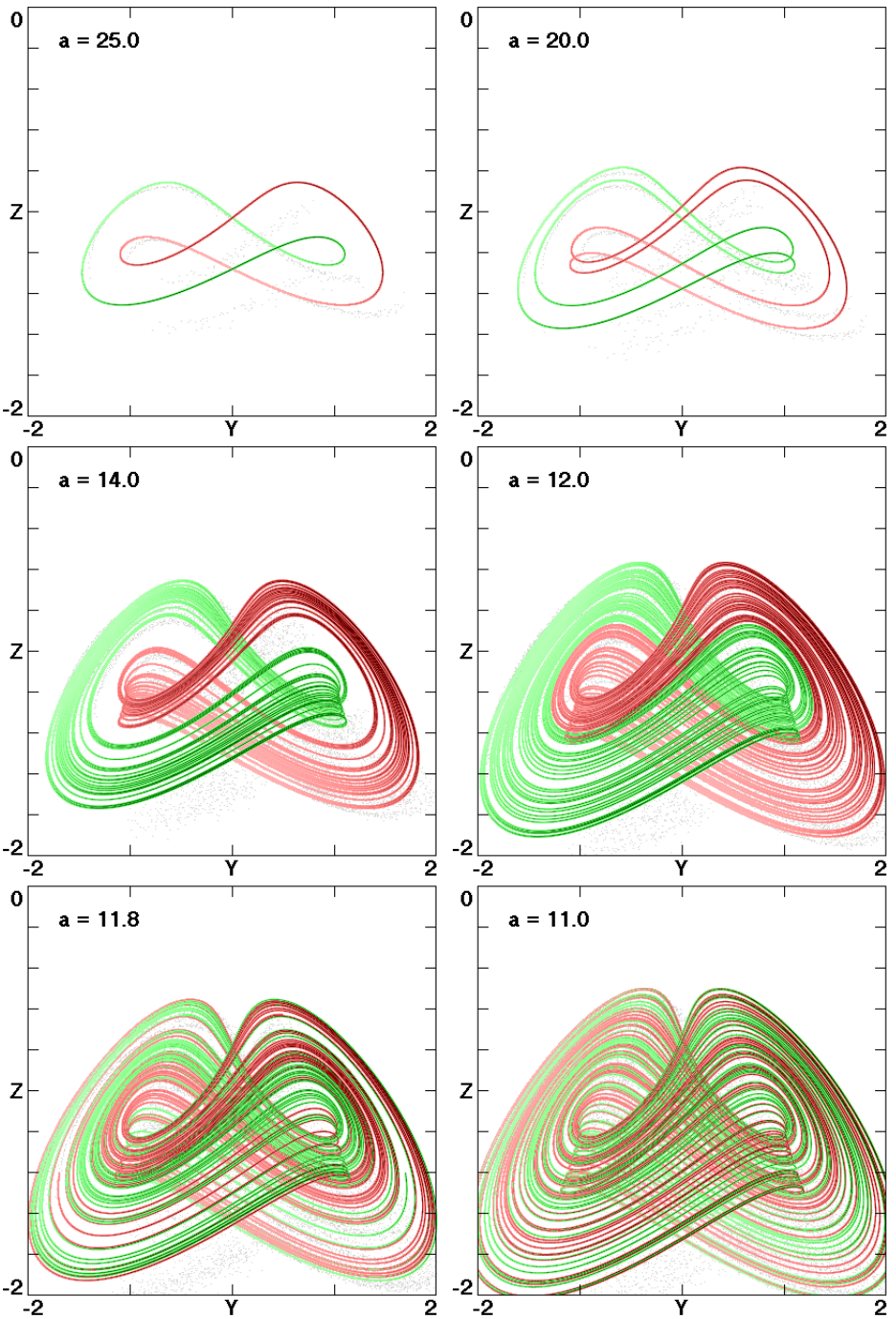

Fig. 4. Bifurcation and merging of the coexisting attractors in system (1) when $b = 0.55$ with initial conditions $(\pm 0.1, 0, -1)$.

and 1.0, respectively. The corresponding basins of attraction are shown in Fig. 8. In Fig. 8(a), the basins of attraction are marked in yellow and green representing the symmetric pair of point attractors. Two coordinate axes are basin boundaries with special dynamical properties. The line $z = 0$ implies $\frac{dy}{dt} = 0$ from Eq. (1) and indicates the line of equilibria, which means that when an initial condition lies on the line, the solution of system (1) will remain at the equilibrium unless a small disturbance allows it to approach one of the two isolated stable points. When $x = 0$, since $y = 0$, Eq. (1) becomes $\frac{dz}{dt} = bz^2$. When $z > 0$, the variable z is attracted to infinity, while for $z < 0$, the variable z is attracted to the fixed point (0, 0, 0), which is an equilibrium point of the system. In Fig. 8(b), the central large area in light blue represents the limit cycle while the region in red indicates a strange attractor. Two

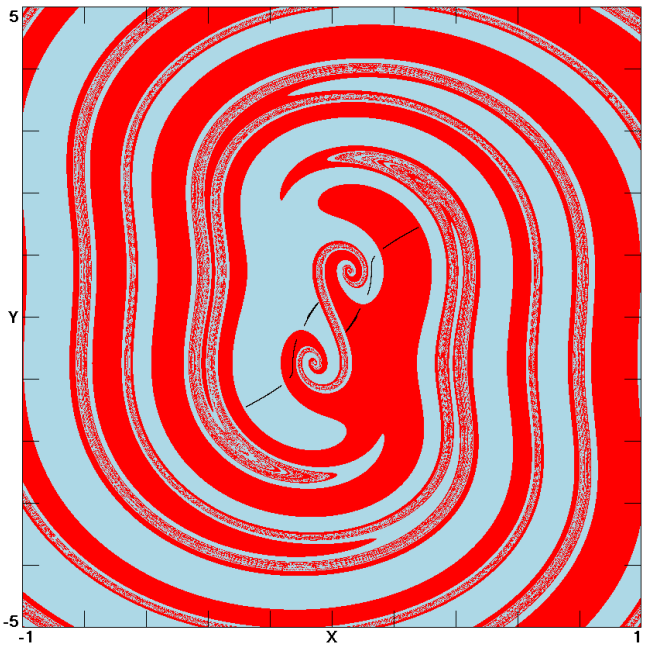

Fig. 5. Basins of attraction in the cross-section $z = -1$ for the symmetric pair of strange attractors for system (1) at $a = 13, b = 0.55$.

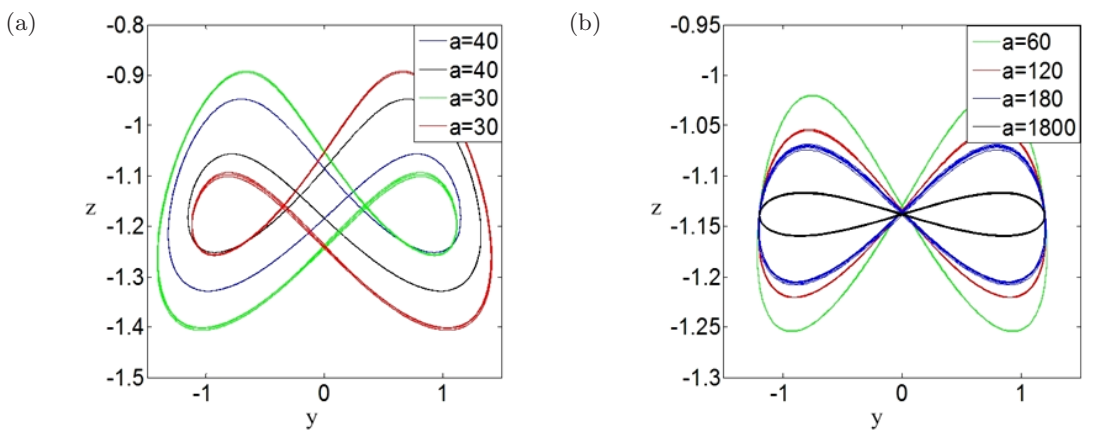

Fig. 6. Two interlinked limit cycles merge into a symmetric one when $b = 0.55$ with initial conditions $(\pm 0.1, 0, -1)$.

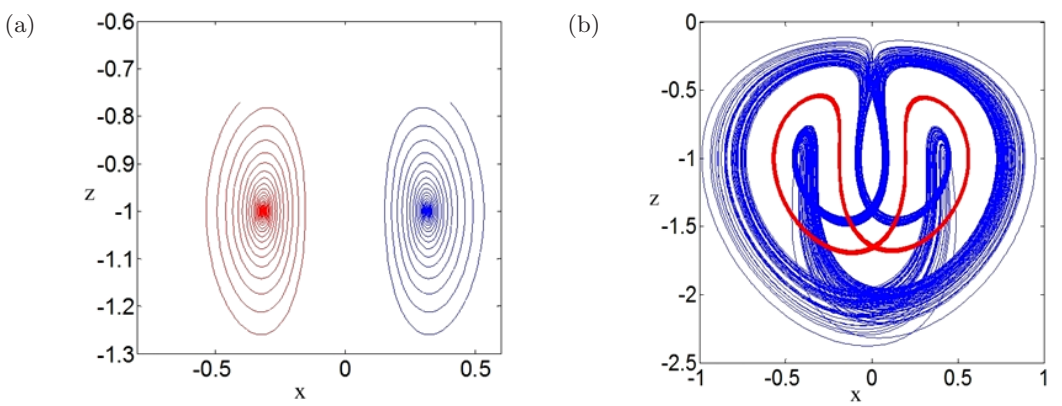

Fig. 7. Other regions of mulitistability: (a) coexisting point attractors when $a = 1, b = 0.1$ with initial conditions $(\pm 0.1, 0, -1)$ and (b) limit cycle coexisting with a strange attractor at $a = 5, b = 0.95$, initial condition $(0.06, 0, -0.5)$ gives chaos, and initial condition $(0.1, -2, -1)$ gives a limit cycle.

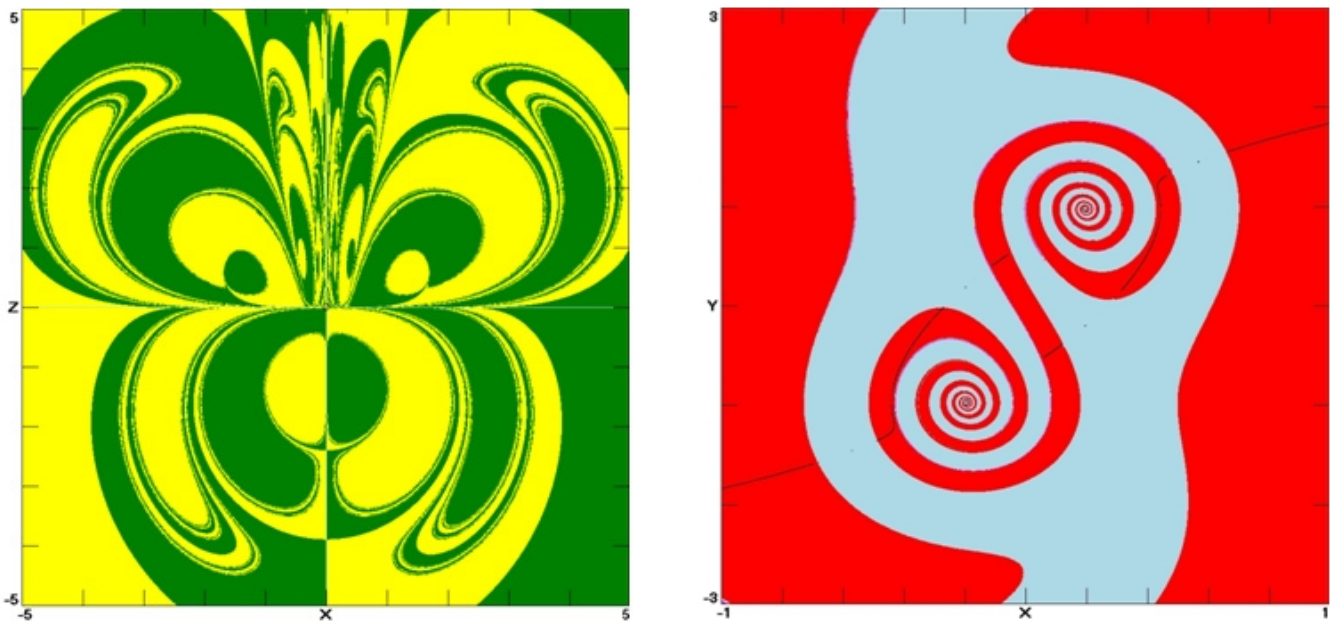

(a) (b)

Fig. 8. Basins of attraction for system (1): (a) cross-section for $y = 0$ when $a = 1, b = 0.1$ and (b) cross-section for $z = -1$ when $a = 5, b = 0.95$.

hollow circles represent the corresponding unstable saddle-foci $(\pm 0.1949, \pm 0.9747, -1)$ with eigenvalues $(-3.2245, 0.1622 \pm 1.7088i)$ showing both coexisting attractors are self-excited rather than hidden [Jiang *et al.*, 2016; Leonov *et al.*, 2011, 2012; Wei & Zhang, 2014; Wei *et al.*, 2014].

4. Amplitude Control with Multistability

Bifurcation parameters affect the dynamic behavior of a system, while amplitude parameters rescale the variables without any bifurcation. Besides the two bifurcation parameters a and b, system (1) has two regimes of amplitude control. The coefficient n in the only linear term y in Eq. (2) is one kind of total amplitude parameter [Li & Sprott, 2013], which controls the amplitude of all the variables. But this parameter changes the frequency and thus the values of the Lyapunov exponents [Li & Sprott, 2014b] as shown by a variable transformation. Let $(x, y, z, t) \to (nx, ny, nz, \frac{t}{n})$. Then Eq. (2) reverts to Eq. (1), which means the parameter n is a controller for both amplitude and frequency.

$$\begin{aligned} \dot{x} &= ny + yz \\ \dot{y} &= yz - axz \\ \dot{z} &= bz^2 - y^2. \end{aligned} \tag{2}$$

The system (1) has another regime of amplitude control. Since system (1) has rotational symmetry, the coefficient m in Eq. (3) of the quadratic term y^2 in the last variable z is a partial amplitude controller and can rescale the variables x and y [Li & Sprott, 2013]. When $(x, y, z) \to (\frac{x}{\sqrt{m}}, \frac{y}{\sqrt{m}}, z)$, Eq. (3) reverts to Eq. (1) implying that the parameter m is an amplitude control parameter for the variables x and y according to $\frac{1}{\sqrt{m}}$.

$$\begin{aligned} \dot{x} &= y + yz \\ \dot{y} &= yz - axz \\ \dot{z} &= bz^2 - my^2. \end{aligned} \tag{3}$$

Note that the multistability makes amplitude control more complicated, and the multistable states can occasionally defeat the amplitude control. In practice it is often difficult to modify the initial condition adaptively when the amplitude parameter is changed, and the inevitable noise may cause the system to cross a basin boundary putting the system into an undesired state. This phenomenon is called an amplitude control crisis.

Suppose there is a p-dimensional system with an amplitude parameter, $\dot{X} = F(a, X)$, where a is an amplitude controller. When $a = a_1$, the basins for coexisting strange attractors are Ω_{11}, $\Omega_{12}, \ldots, \Omega_{1m}$ and the basins for other nonchaotic

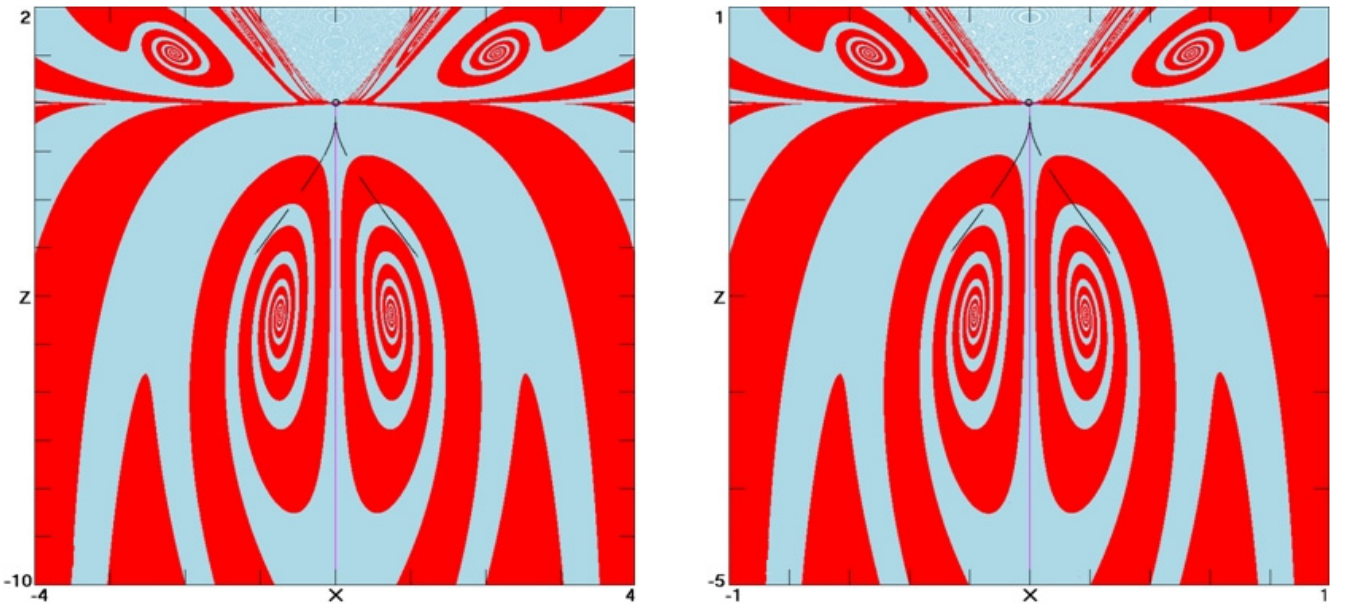

(a) (b)

Fig. 9. Rescaled basins of attraction for system (1) with $a = 5, b = 0.95$ on cross-section $y = 0$: (a) basin expansion when $n = 2$ in Eq. (3) and (b) basin shrink when $m = 4$ in Eq. (4).

attractors are $\Pi_{11}, \Pi_{12}, \ldots, \Pi_{1n}$. These two kinds of basins become $\Omega_{21}, \Omega_{22}, \ldots, \Omega_{2m}$ and $\Pi_{21}, \Pi_{22}, \ldots, \Pi_{2n}$ when $a = a_2$. Let $D_{ij} = \Omega_{1i} \cap \Pi_{2j} (1 \leq i \leq m, 1 \leq j \leq n)$, if the initial condition is set as $X_0 = (x_{10}, x_{20}, \ldots, x_{p0}) \in D_{ij}$, when the amplitude parameter a increases from a_1 to a_2, the largest Lyapunov exponent can switch from positive to zero if a basin boundary is crossed between a strange attractor and a limit cycle. This is caused by the shrink or expansion in the basin of attraction when the parameter rescales the amplitude. For example, the parameter n in system (3) expands the basin in three dimensions according to n (if $n > 1$) in initial space while the parameter m in system (4) shrinks the basin in two dimensions of x and y according to $\frac{1}{\sqrt{m}}$ (if $m > 1$). As shown in Fig. 9, the basin is extruded and the size gets doubled in both dimensions when $n = 2$, while the basin is compressed only in the direction of x-axis when $m = 4$ compared with the original basins. Therefore, a fixed initial condition may "visit" different parts due to the basin motion caused by the amplitude control. To show it more clearly, suppose there are three regions corresponding to three different dynamical behaviors: chaos, limit cycle and point attractor, as shown in Fig. 10. We assume that a fixed initial condition (red dot) is in the middle of basin of limit

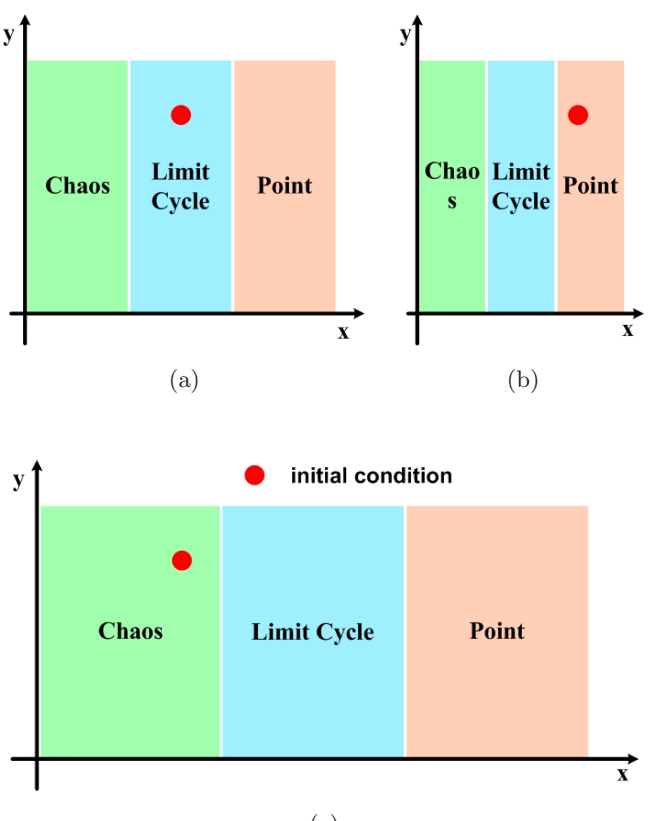

(a) (b) (c)

Fig. 10. Fixed initial condition visits different basins of attraction when an amplitude parameter rescales the basins.

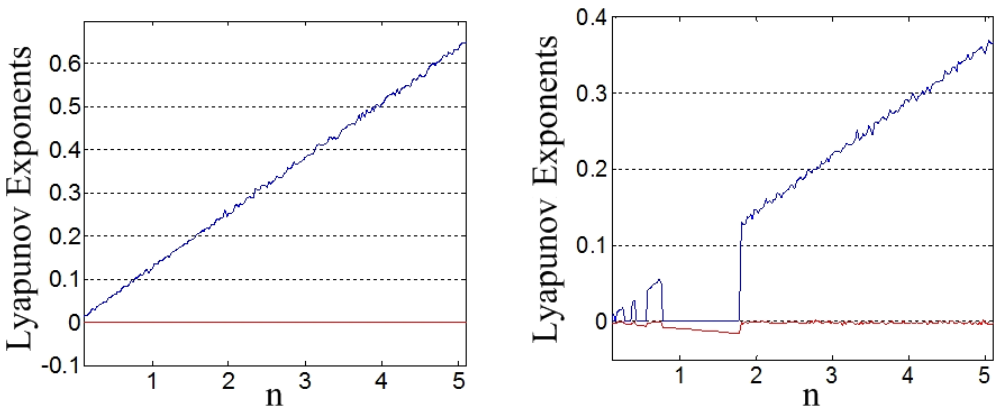

(a) (b)

Fig. 11. Lyapunov exponents when n varies with initial condition $(0, 0.4, -1)$: (a) $a = 5.5, b = 0.55$ and (b) $a = 5, b = 0.95$.

cycle [Fig. 10(a)]. If a parameter rescales the variable x without modifying the variables y and z, the basin will be compressed [Fig. 10(b)] or stretched [Fig. 10(c)], correspondingly the initial condition will go forward to the basin of point attractor or retreat back to the basin of chaotic attractor triggering a "state-fly" in the system. The sensitivity of state-fly is related to the location of the initial condition, the area of the basins for different dynamics and the rescaled basins caused by the amplitude parameter. Specifically, if the basins do not change dramatically and the initial condition stays in the same basin of attraction, the system will not yield a state-fly.

As shown in Fig. 11(a), when the bifurcation parameters a and b and the initial conditions are fixed, the Lyapunov exponents will increase linearly with the amplitude controller n since it also increases the oscillation frequency linearly. But when the system has different kinds of coexisting attractors, as shown in Fig. 11(b), the occurrence of "state-fly" with the amplitude control causes a discontinuity in the Lyapunov exponents when a basin boundary is crossed. Such jumps can be used to detect multistability [Li & Sprott, 2014c].

As shown in Fig. 12(a), selecting the parameters a and b for monostable chaos, Lyapunov exponents will remain unchanged when the partial amplitude parameter m varies. When the system has multistable states, as shown in Fig. 12(b), notches in the Lyapunov exponent spectrum indicate that the same initial condition crosses basin boundaries for different attractors. Due to the different control intensity of the amplitude parameters

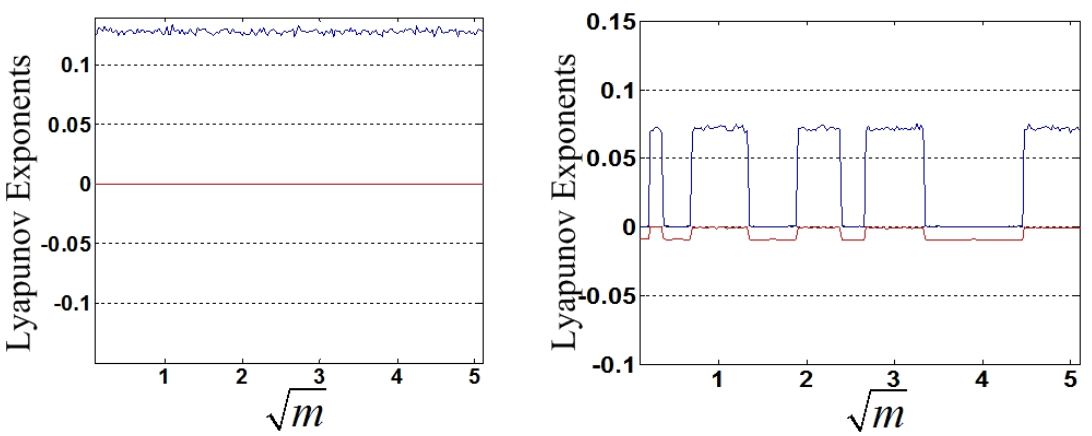

(a) (b)

Fig. 12. Lyapunov exponents when m varies with initial condition $(1, 0.4, -1)$: (a) $a = 5.5, b = 0.55$ and (b) $a = 5, b = 0.95$.

m and n, we let the partial amplitude controller m vary from 0 to 25 in order to get a better observation of the switches between states. For the same reason, the initial value x_0 is set to a nonzero value to ensure that the line of equilibria is not selected as the initial condition since it will shield the effect of the amplitude parameter.

Note that a fundamental property of a chaotic system is its sensitive dependence on initial conditions. Even two close initial conditions may cause the phase trajectories to separate exponentially with time, and the Lyapunov exponent is a quantitative measure of this sensitivity. However, in multistable chaotic systems, the sensitivity to initial conditions depends on the basin of attraction which contains the initial conditions. Because different basins are associated with different solutions, only those initial conditions in the basin of a strange attractor have sensitivity leading to a butterfly effect. When the initial condition is in the basin of a nonchaotic attractor, the sensitivity will disappear. Amplitude parameters determine the size of the basin of attraction, and therefore determine the range of sensitivity. Amplitude parameters change the amplitude of the signal while not changing statistical properties of the system. Thus the amplitude controller is mainly applied in chaotic circuits [Li *et al.*, 2015b; Li *et al.*, 2012] and other information systems [Liu *et al.*, 2007; Chen *et al.*, 2014; Chen *et al.*, 2015]. When the amplitude parameter is modulated by a slowly varying signal or other chaotic code, the newly generated chaotic sequences will have stronger random performance, which will be the subject of future research.

5. Discussions and Conclusions

Amplitude control of chaotic signals is sometimes accompanied by alteration of the frequency, and therefore there are two regimes of amplitude control, one of which only revises the amplitude of the variable partially or totally, while the other rescales the amplitude and the frequency of the signals. In this paper, a case of a chaotic system with both regimes of amplitude control is proposed, which has other unique properties of multistability, offering a good opportunity to observe the crisis in amplitude control. The space of initial conditions is divided as different basins of attraction associated with different dynamical behavior. An amplitude parameter will rescale the basins of attraction, and consequently a fixed or noise-influenced initial condition may jump between basins of attraction, which drives the system to different states and causes a crisis for engineering application.

Acknowledgments

This work was supported financially by the Startup Foundation for Introducing Talent of NUIST (Grant No.: 2016205), the Natural Science Foundation of the Jiangsu Higher Education Institutions of China (Grant No.: 16KJB120004), the Advantage Discipline Information and Communication Engineering of Jiangsu Province, the National Natural Science Foundation of China (Grant No.: 61072133) and a Project Funded by the Priority Academic Program Development of Jiangsu Higher Education Institutions.

References

Bao, B., Li, Q., Wang, N. & Xu, Q. [2016] "Multistability in Chua's circuit with two stable node-foci," *Chaos* **26**, 043111.

Barrio, R., Blesa, F. & Serrano, S. [2009] "Qualitative analysis of the Rössler equations: Bifurcations of limit cycles and chaotic attractors," *Physica D* **238**, 1087–1100.

Chen, D., Zhang, R., Sprott, J. C., Chen, H. & Ma, X. [2012a] "Synchronization between integer-order chaotic systems and a class of fractional-order chaotic systems via sliding mode control," *Chaos* **22**, 023130.

Chen, D., Zhang, R., Sprott, J. C., Chen, H. & Ma, X. [2012b] "Synchronization between integer-order chaotic systems and a class of fractional-order chaotic system based on fuzzy sliding mode control," *Nonlin. Dyn.* **70**, 1549–1561.

Chen, J., Li, J., Li, P., Zhu, Y. & Long, W. [2014] "Joint DOD and DOA estimation for high-speed target using bistatic MIMO radar," *Int. J. Antenn. Propag.*, doi: 10.1155/2014/914327.

Chen, J., Li, P., Zhu, Y. & Li, J. [2015] "Parameter estimation method for high-speed target using bistatic MIMO radar with dual-frequency transmitters," *Wireless Pers. Commun.* **85**, 2083–2098.

Jafari, S. & Sprott, J. C. [2013] "Simple chaotic flows with a line equilibrium," *Chaos Solit. Fract.* **57**, 79–84.

Jiang, H., Liu, Y., Wei, Z. & Zhang, L. [2016] "Hidden chaotic attractors in a class of two-dimensional maps," *Nonlin. Dyn.* **85**, 2719–2727.

Kuznetsov, N. V. [2016] "The Lyapunov dimension and its estimation via the Leonov method," *Phys. Lett. A* **380**, 2142–2149.

Kuznetsov, N. V., Alexeeva, T. A. & Leonov, G. A. [2016] "Invariance of Lyapunov exponents and Lyapunov dimension for regular and irregular linearizations," *Nonlin. Dyn.* **85**, 195–201.

Leonov, G. A., Vagaitsev, V. I. & Kuznetsov, N. V. [2011] "Localization of hidden Chua's attractors," *Phys. Lett. A* **375**, 2230–2233.

Leonov, G. A., Vagaitsev, V. I. & Kuznetsov, N. V. [2012] "Hidden attractor in smooth Chua systems," *Physica D* **241**, 1482–1486.

Leonov, G. A., Kuznetsov, N. V., Korzhemanova, N. A. & Kusakin, D. V. [2016] "Lyapunov dimension formula for the global attractor of the Lorenz system," *Commun. Nonlin. Sci. Numer. Simulat.* **41**, 84–103.

Li, C. & Wang, D. [2009] "An attractor with invariable Lyapunov exponent spectrum and its jerk circuit implementation," *Acta Phys. Sin.* (*Chinese Edition*) **58**, 764–770.

Li, C., Wang, H. & Chen, S. [2010] "A novel chaotic attractor with constant Lyapunov exponent spectrum and its circuit implementation," *Acta Phys. Sin.* (*Chinese Edition*) **59**, 783–791.

Li, C., Wang, J. & Hu, W. [2012] "Absolute term introduced to rebuild the chaotic attractor with constant Lyapunov exponent spectrum," *Nonlin. Dyn.* **68**, 575–587.

Li, C. & Sprott, J. C. [2013] "Amplitude control approach for chaotic signals," *Nonlin. Dyn.* **73**, 1335–1341.

Li, C. & Sprott, J. C. [2014a] "Multistability in the Lorenz system: A broken butterfly," *Int. J. Bifurcation and Chaos* **24**, 1450131-1–7.

Li, C. & Sprott, J. C. [2014b] "Chaotic flows with a single nonquadratic term," *Phys. Lett. A* **378**, 178–183.

Li, C. & Sprott, J. C. [2014c] "Finding coexisting attractors using amplitude control," *Nonlin. Dyn.* **78**, 2059–2064.

Li, C., Sprott, J. C., Yuan, Z. & Li, H. [2015a] "Constructing chaotic systems with total amplitude control," *Int. J. Bifurcation and Chaos* **25**, 1530025-1–14.

Li, H., Li, C., Yuan, Z., Hu, W. & Zheng, X. [2015b] "A new class of chaotic circuit with logic elements," *J. Circuit. Syst. Comp.* **24**, 1550136.

Li, C., Pehlivan, I. & Sprott, J. C. [2015c] "A novel four-wing strange attractor born in bistablity," *IEICE Electron. Expr.* **12**, 1–12.

Li, C., Sprott, J. C. & Xing, H. [2016a] "Hypogenetic chaotic jerk flows," *Phys. Lett. A* **380**, 1172–1177.

Li, C., Sprott, J. C. & Xing, H. [2016b] "Constructing chaotic systems with conditional symmetry," *Nonlin. Dyn.*, doi: 10.1007/s11071-016-3118-1.

Liu, Z., Zhu, X., Hu, W. & Jiang, F. [2007] "Principles of chaotic signal radar," *Int. J. Bifurcation and Chaos* **17**, 1735–1739.

Sprott, J. C. [2000] "A new class of chaotic circuit," *Phys. Lett. A* **266**, 19–23.

Sprott, J. C. [2011] "A new chaotic jerk circuit," *IEEE Trans. Circuits Syst.-II*: *Exp. Briefs* **58**, 240–243.

Sprott, J. C., Wang, X. & Chen, G. [2013] "Coexistence of point, periodic and strange attractors," *Int. J. Bifurcation and Chaos* **23**, 1350093-1–5.

Sprott, J. C. [2014] "Simplest chaotic flows with involutional symmetries," *Int. J. Bifurcation and Chaos* **24**, 1450009-1–9.

Sprott, J. C., Wang, X. & Chen, G. [2014] "When two dual chaotic systems shake hands," *Int. J. Bifurcation and Chaos* **24**, 1450086-1–3.

Strogatz, S. H. [1994] *Nonlinear Dynamics and Chaos, with Applications to Physics, Biology, Chemistry and Engineering* (Addison-Wesley Publishing Company, New Jersey).

Wei, Z., Wang, R. & Liu, A. [2014] "A new finding of the existence of hidden hyperchaotic attractors with no equilibria," *Math. Comput. Simulat.* **100**, 13–23.

Wei, Z. & Zhang, W. [2014] "Hidden hyperchaotic attractors in a modified Lorenz–Stenflo system with only one stable equilibrium," *Int. J. Bifurcation and Chaos* **24**, 1450127-1–14.

Wolf, A., Swift, J. B., Swinney, H. L. & Vastano, J. A. [1985] "Determining Lyapunov exponents from a time series," *Physica D* **16**, 285–317.

Xu, Q., Lin, Y., Bao, B. & Chen, M. [2016] "Multiple attractors in a non-ideal active voltage-controlled memristor based Chua's circuit," *Chaos Solit. Fract.* **83**, 186–200.

Yu, S., Lü, J., Chen, G. & Yu, X. [2011] "Generating grid multi-wing chaotic attractors by constructing heteroclinic loops into switching systems," *IEEE Trans. Circuits Syst.-II*: *Exp. Briefs* **58**, 314–318.

Yu, S., Lü, J., Chen, G. & Yu, X. [2012] "Generating grid multi-wing chaotic attractors by constructing heteroclinic loops into switching systems," *IEEE Trans. Circuits Syst.-I*: *Fund. Th. Appl.* **59**, 1015–1028.

Zhang, R. & Yang, S. [2011] "Adaptive synchronization of fractional-order chaotic systems via a single driving variable," *Nonlin. Dyn.* **66**, 831–837.

Zhang, R. & Yang, S. [2012] "Robust chaos synchronization of fractional-order chaotic systems with unknown parameters and uncertain perturbations," *Nonlin. Dyn.* **69**, 983–992.